On the formation of pure and Pt-doped iron silicides using ball milling

2001 J. Phys.: Condens. Matter 13 2737

(http://iopscience.iop.org/0953-8984/13/11/327)

INSTITUTE OF PHYSICS PUBLISHING JOURNAL OF PHYSICS: CONDENSED MATTER

J. Phys.: Condens. Matter **13** (2001) 2737–2747 www.iop.org/Journals/cm PII: S0953-8984(01)14702-8

On the formation of pure and Pt-doped iron silicides using ball milling

J Desimoni and F H Sánchez

Departamento de Física, Facultad de Ciencias Exactas, UNLP, C C No 67, 1900 La Plata, Argentina

E-mail: desimoni@venus.fisica.unlp.edu.ar

Received 12 June 2000

Abstract

The sequence of phase formations for elemental powders of stoichiometric $FeSi_2$ and $Fe_{1-x}Pt_xSi_2$ ($0.03 \leqslant x \leqslant 0.50$) mixtures prepared by mechanical alloying at room temperature in an Ar atmosphere in a horizontal mill is presented. Sample evolution was followed by means of Mössbauer spectroscopy and x-ray diffraction. After the milling, the results indicate the formation of different disordered iron silicides, depending on milling time. The kinetics of iron silicide formation was also studied; a diffusion-controlled process with decreasing nucleation rate was found. In the case of Pt-doped samples, the segregation of Pt silicides was observed even for the smallest concentration, and no noticeable incorporation of Pt into the β-$FeSi_2$ lattice could be inferred. Samples were also subjected to annealing at 1123 K for 4 h to produce ordering in the structures.

1. Introduction

The Fe–Si system is intricate because several stable and metastable phases can be produced depending on the experimental conditions of synthesis. Non-equilibrium processing techniques like ion beam mixing and mechanical alloying allow the formation of compounds and metastable phases. In both cases, energy is supplied to the system under study in the form of mechanical energy. Some portion of this energy is expended to overcome the chemical barriers and to create defects and distortions. When starting from the elemental powder mixture of Fe and Si for ball milling, or Si and Fe layers for ion beam mixing and laser-induced quenching, it is possible to form different phases depending on composition, deposition energy and temperature. For instance, ion beam mixing and laser quenching of equiatomic Fe–Si multilayers induce the formation of a mixture of equiatomic disordered and ordered structures [1–3]. On the other hand, the 380 keV Xe^+ irradiation of a Fe layer deposited on (100) Si leads to the formation of Fe_3Si, FeSi and β-$FeSi_2$ when the substrate temperature is kept at $T \leqslant 573$ K, while for higher substrate temperatures α-$FeSi_2$ is formed additionally [2]. In samples prepared by mechanical alloying, a discrepancy has been reported concerning

0953-8984/01/112737+11$30.00

the sequence of phase formations. According to reference [4], α-$FeSi_2$ was not detected, and the formation of β-$FeSi_2$ took place throughout a reaction between ε-FeSi and Si. In other experiments [5], instead of β-$FeSi_2$, the formation of α-$FeSi_2$ together with ε-FeSi was observed and it was postulated that α-$FeSi_2$ reacts with ε-FeSi to give rise to β-$FeSi_2$.

The semiconducting β-$FeSi_2$ phase has attracted attention because its thermoelectric properties can be changed by doping with metallic atoms. For instance, the material has p-type properties if doped with Mn atoms and n-type properties if doped with Pt atoms [6]. The structure of β-$FeSi_2$ is a complex one having, per unit cell, 32 silicon atoms and 16 iron atoms, the latter in two non-equivalent sites (site I and site II), equally populated [7]. The localization of impurity atoms in the lattice sites is still an open question. Recently, a new model for the assignment of the measured hyperfine interactions to the Fe sites has been reported [8]. This model could help us to understand the impurity localization in the lattice of β-$FeSi_2$.

Experiments dealing with the sequence of phase formations of $FeSi_2$ and $Fe_{1-x}Pt_xSi_2$ ($0.03 \leqslant x \leqslant 0.50$) systems after mechanical alloying at room temperature in Ar atmosphere are presented. The sample evolution with milling time and Pt concentration was followed by means of Mössbauer spectroscopy and x-ray diffraction. The phase formation after annealing at 1123 K for four hours is also discussed.

2. Experimental procedure

Mixtures (0.700 g) of stoichiometric amounts of elemental Fe (99.999% purity) and Si (99.99% purity) for pure silicides and Fe, Si and Pt (99.95% purity) for $Fe_{1-x}Pt_xSi_2$, were mechanically alloyed at room temperature in an Ar atmosphere using a Restsch MM2 horizontal mill operated at 33 Hz. The ball-to-powder ratio was 10:1.

Samples were characterized by means of x-ray diffraction (XRD) in a Philips PW1710 diffractometer using graphite-monochromatized Cu Kα radiation. Data were recorded in the range $10^\circ \leqslant 2\theta \leqslant 110^\circ$ in steps of 0.02° with a counting time of 2 s per step. Phase identification was performed using the *Powder Diffraction Files* [9].

Mössbauer spectra were taken in transmission geometry using a ^{57}Co**Rh** source of approximately 5 mCi activity and recorded in a standard 512-channel conventional constant-acceleration spectrometer. Two sets of spectra were taken in order to analyse in detail the different phases present in the samples. In one case the velocity range ran between -8 and +8 mm s^{-1} and in the other one it was between -2 and +2 mm s^{-1}. Velocity calibration was performed with a 12 μm thick α-Fe foil. All spectra were fitted to Lorentzian line shapes with a non-linear least-squares program with constraints. The isomer shifts are referred to α-Fe at 298 K.

The annealings at 1123 K for 4 h inside quartz ampoules ($p \approx 5 \times 10^{-6}$ mbar) were carried out with a conventional electric oven.

3. Results and discussion

The kinetics of formation of iron silicides, as well as the end products, were investigated by means of x-ray diffraction and Mössbauer spectroscopy in samples with $FeSi_2$ composition. The diffractograms of the as-milled samples, shown in figure 1, are characterized by broad lines, associated with grain refinement and lattice internal strain. An admixture of phases was identified, while amorphous phases were not observed. For milling times shorter than 4 h, the lines belonging to Si and Fe are observed. The contribution to the diffractograms of these lines

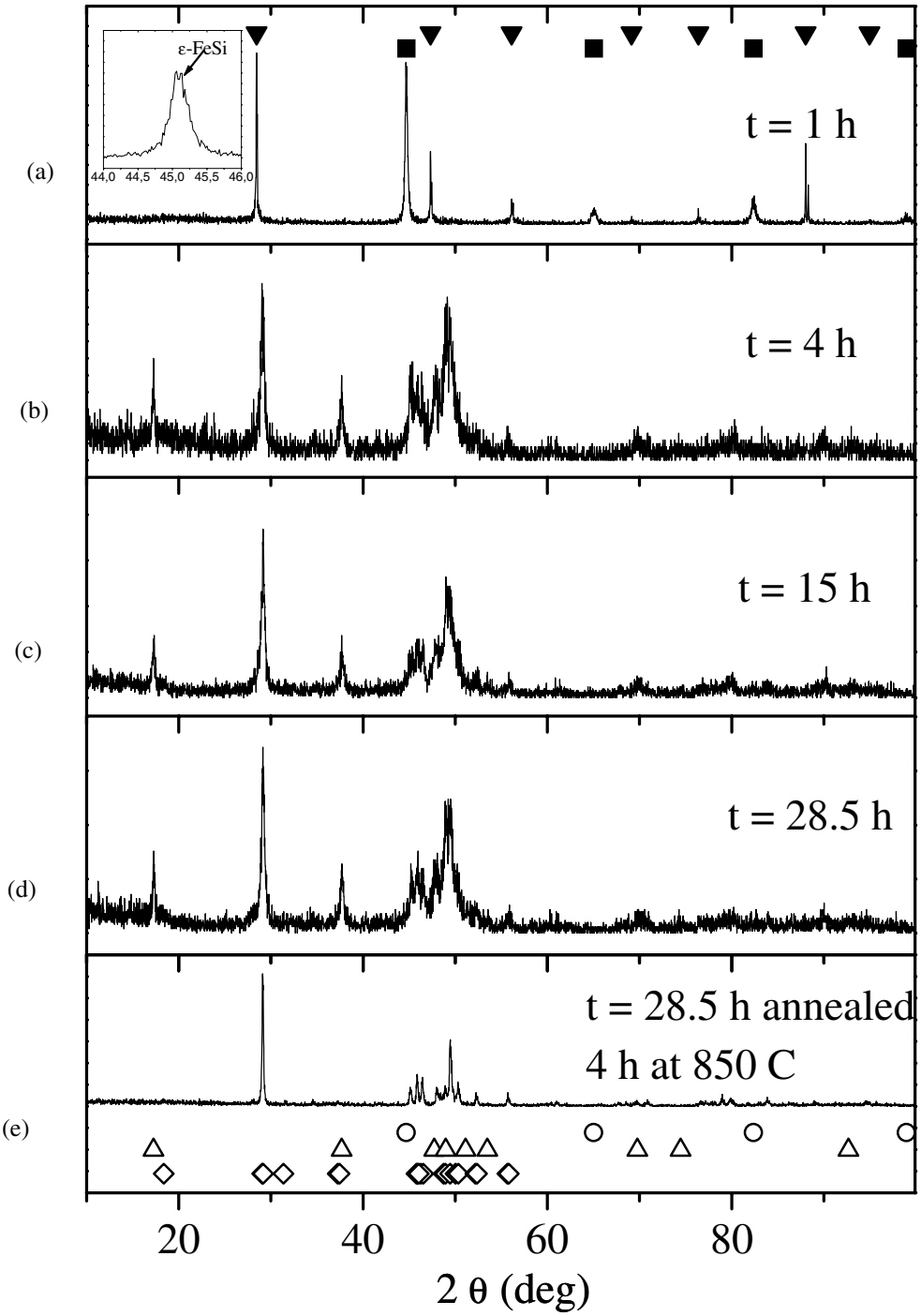

Figure 1. X-ray diffractograms of $FeSi_2$ mixtures subjected to milling for different times: (a) $t = 1$ h, (b) $t = 4$ h, (c) $t = 15$ h, (d) $t = 28.5$ h and (e) $t = 28.5$ h and annealed at 1173 K for 4 h. The solid squares and triangles indicate the positions of α-Fe and Si lines, respectively. The open circles, triangles and diamonds indicate the positions of the lines belonging to ε-FeSi, α-$FeSi_2$ and β-$FeSi_2$, respectively.

gradually decreases with milling time. After 1 h of milling, traces of ε-FeSi, as observed in the inset of figure 1(a)), are detected, indicating that this silicide is the first product formed. For larger milling times, other silicides are also present in the samples; the lines displayed in the diffractograms can be ascribed to α-$FeSi_2$, β-$FeSi_2$ and ε-FeSi. The presence of the last phase is more important at short times, while the contribution of β-$FeSi_2$ reaches a maximum after 4 h of milling and then remains constant.

For times up to 4 h of milling, Mössbauer spectra with a wide velocity range (not shown here) are characterized by two central lines superimposed onto the α-Fe sextet ($B = 33_1$ T, $\delta = 0.00_1$ mm s^{-1}) whose intensity decreases with milling time. The relative fraction of α-Fe (F_α) is quoted in table 1. The central lines can be ascribed to the disordered iron silicide phases [10]. In agreement with the XRD results, for milling times higher than 4 h the contribution of the sextet to the spectra is null. After the completion of the reaction between Fe and Si atoms, no changes are noticed either in the diffractograms or in the Mössbauer spectra, indicating that once the elemental powders are completely consumed, a dynamic equilibrium between the phases is reached, i.e. a steady state is achieved.

Table 1. Hyperfine parameters (Δ_i = quadrupole splitting, δ_i = isomer shift and Γ_i = linewidth) and relative fractions (F_i) for $FeSi_2$ mixtures subjected to milling for different times.

Time (h)	Δ_1 (mm s^{-1})	δ_1 (mm s^{-1})	Γ_1 (mm s^{-1})	F_1 (%)	Δ_2 (mm s^{-1})	δ_2 (mm s^{-1})	Γ_2 (mm s^{-1})	F_2 (%)	F_α (%)
1†	0.60_3	0.24_2	0.48_5	11_1					89_3
1.5†	0.53_1	0.28_1	0.37_1	19_1	0.51_1	0.10_1	0.38_2	26_4	55_2
2†	0.53_1	0.22_1	0.41_1	23_3	0.531	0.141	0.401	35_4	42_3
2.5†	0.54_1	0.28_1	0.39_1	26_3	0.51_1	0.10_1	0.42_1	26_3	48_1
3	0.54_1	0.26_1	0.38_1	47_4	0.59_1	0.12_2	0.42_1	46_4	6_1
4	0.55_1	0.28_1	0.40_1	42_2	0.50_1	0.08_1	0.42_1	58_2	
6.83	0.55_1	0.26_1	0.41_1	49_3	0.53_1	0.09_1	0.46_1	48_4	
15	0.58_1	0.27_1	0.41_1	31_1	0.49_1	0.08_1	0.41_1	69_1	
16	0.56_1	0.26_1	0.41_1	51_2	0.50_1	0.09_1	0.42_1	49_2	
19	0.58_1	0.28_1	0.41_1	42_1	0.50_1	0.09_1	0.42_1	58_1	
27.5	0.57_1	0.27_1	0.41_2	37_2	0.50_1	0.08_1	0.42_1	63_2	
28.5	0.57_1	0.26_1	0.42_1	41_2	0.51_1	0.08_1	0.40_1	59_2	
55	0.56_1	0.27_1	0.41_1	37_1	0.49_1	0.09_1	0.41_1	62_1	

† Values averaged over experiments on several independent samples.

The evolution of the silicide relative fraction ($f(t) = F_1 + F_2$ of table 1) with milling time is displayed in figure 2. An increase of the silicide contribution is observed; it is saturated at 100% after approximately 5 h of milling. The silicide relative fraction evolution follows a sigmoidal behaviour, typical of a nucleation-and-growth reaction; the kinetics of the transformation was analysed using the Avrami equation [11]:

$$f(t) = 1 - \exp(-kt^n).$$

The mechanism of the transformation is determined by the kinetics parameters n and k. The time exponent n is related to the particular nucleation-and-growth conditions, while the constant rate of the reaction k is associated with the rate of nucleation and growth of the new phase. These kinetics parameters were determined by fitting the curve, and the resulting values are $n = 2.0 \pm 0.4$ and $k = 0.19 \pm 0.06$ s^{-1}. The n-value indicates a diffusion-controlled growth with decreasing nucleation rate.

In the early stage of the milling process, the elemental powders welded together giving rise to the formation of an Fe/Si interface and a decrease in the crystallite size. According

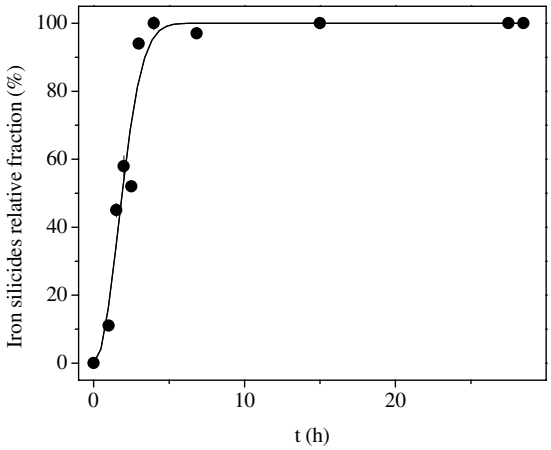

Figure 2. Evolution with milling time of the iron silicide relative fraction. The solid line is the result of the fit to the data with an Avrami-type equation.

to Umemoto *et al* [4], mechanical alloying is a random walk and the resulting structure is similar to those expected from the diffusion of both species. This hypothesis is confirmed by the present results, through the determination of the kinetics of formation of silicides. In this framework, it could be possible to assume that the atomic transport is diffusion-like with a diffusion coefficient enhanced by the deposited energy of the process itself and a chemical driving force originating from the negative heat of mixing [12].

In order to investigate in detail the central part of the Mössbauer spectra, the velocity range of the spectrometer was set at $[-2, 2\ \text{mm s}^{-1}]$. The spectra, characterized by broad lines suggesting a high degree of disorder in the phases (see figure 3), were reproduced with two interactions except for $t = 1$ h. For this milling time, the smallness of the contribution to the spectrum of the quadrupole signal prevented us from identifying more than one Fe site. For times shorter than 4 h, the two central lines of the α-Fe sextet are also observed in the spectra. The results of the fits are reported in table 1.

Currently there is wide consensus on how the β-$FeSi_2$ and ε-FeSi Mössbauer spectra must be interpreted. That of β-$FeSi_2$ consists of two unresolved, equally populated, quadrupole interactions with similar isomer shifts and different quadrupole splittings, while that of ε-FeSi corresponds to only one quadrupole interaction. On the other hand, though the pattern of α-$FeSi_2$ is well known (a rather wide asymmetric doublet with different component linewidths), quite different approaches have been used to reproduce it (see table 2).

The fitted hyperfine parameters (table 1) and the x-ray results indicate that the first phase produced is ε-FeSi. After that, silicides with $FeSi_2$ stoichiometry are also formed, probably highly disordered. Therefore, it can be assumed that the first interaction reported in table 1 mostly originates from the ε-FeSi phase. The isomer shift of the second interaction is close to that of the average of the β-$FeSi_2$ ones. We have thus assumed that the main contribution to this interaction comes from the β-phase in spite of its quadrupole splitting ($\approx$0.5 mm s^{-1}) being larger than the β-$FeSi_2$ average ($\approx$0.4 mm s^{-1}), since this quantity is strongly sensitive to small local departures from crystal symmetry while the isomer shift is not. According to the x-ray results, α-$FeSi_2$ is also present; hence its contribution to the spectra must be shared by the two interactions reported in table 1. Thus, due to the phase and hyperfine parameter superposition, it is not possible to perform a unique assignment of the fitted interactions to the different phases [10].

Two different mechanisms of phase formation under mechanical alloying in systems with initial composition $FeSi_2$ have been reported [4, 5]. According to Umemoto *et al* [4], it is

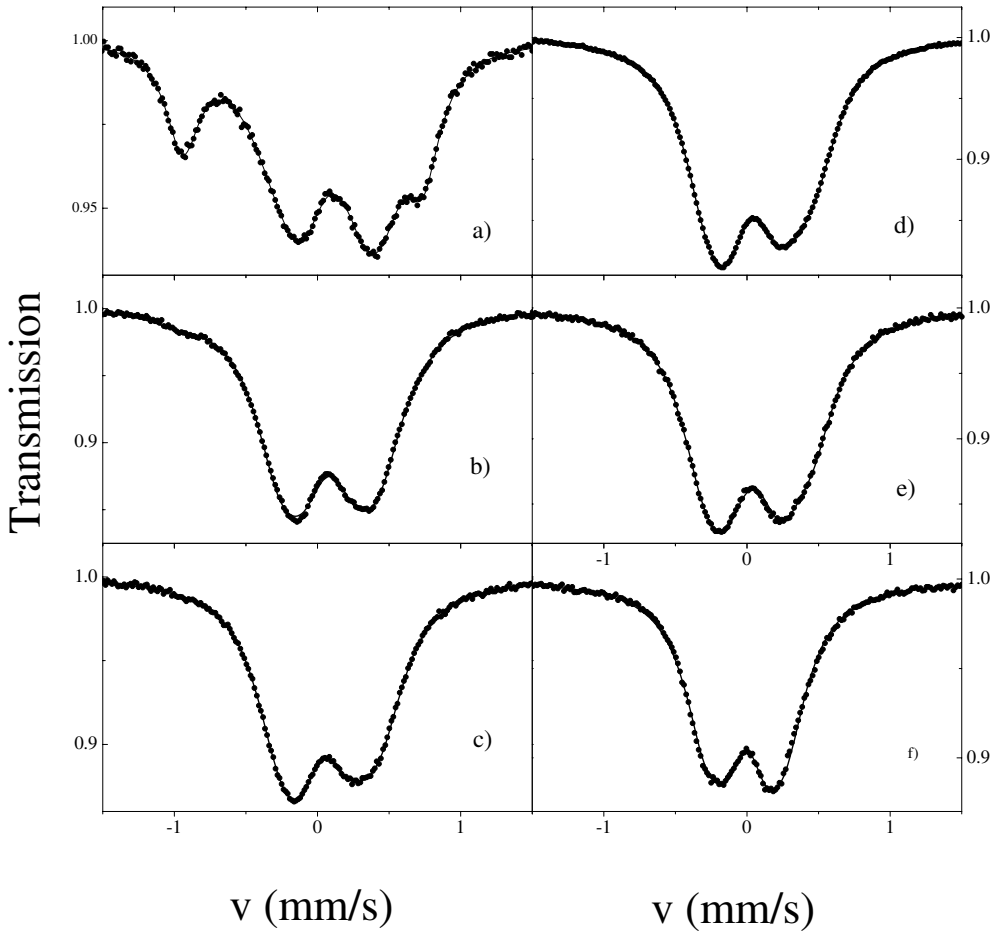

Figure 3. Narrow-velocity-range Mössbauer-effect spectra recorded from $FeSi_2$ mixtures milled for different times: (a) $t = 3$ h, (b) $t = 6.8$ h, (c) $t = 16$ h, (d) $t = 19$ h, (e) $t = 28.5$ h and (f) $t = 28.5$ h and annealed at 1173 K for 4 h.

possible to synthesize β-$FeSi_2$, avoiding the formation of ε-FeSi, by milling for a short time and annealing. Samples prepared using a planetary mill, at highest-energy conditions, after Gaffet *et al* [5], give end products corresponding to a mixture of Fe, Si, FeSi, α-$FeSi_2$ and amorphous phases. Crystalline phases were also observed for lower-energy conditions and lower duration times. In the present experiments, ε-FeSi is formed alone after short times and, subsequently, ε-FeSi, α-$FeSi_2$ and β-$FeSi_2$ are present at the same time. Moreover, when the initial powders are consumed, i.e. neither Fe nor Si atoms remain without reacting, the three phases remain present with contributions independent of the time of milling.

According to Schwartz [20], it is not possible to mechanically alloy mixtures of metal and metalloid powders. This hypothesis is based on the fact that the mechanical attrition for milling breaks the metalloid into nanosized particles which are dispersed throughout the metal phase, preferentially at grain boundaries, but alloying does not occur. The formation of intermetallic phases is expected after annealing at moderate temperatures. However, this is not the case for the Fe–Si system, which is prone to form stable and metastable compounds, depending on the milling conditions.

Table 2. Hyperfine interactions reported in the literature for ε-FeSi, β-$FeSi_2$ and α-$FeSi_2$.

Phase	Iron site	δ (mm s^{-1})	Δ (mm s^{-1})	Reference
ε-FeSi	Fe I	0.28_2	0.50_2	[13, 14]
β-$FeSi_2$	Fe I	0.076_8	$+0.525_8$	[8, 15]
	Fe II	0.091_8	-0.315_8	
α-$FeSi_2$	Fe I	0.27	0.49	[14]
	Fe I	0.2†	0.55†	[16]
	Fe I	0.23	0.47	[17]
	Fe II	0.26	0.73	
	$Fe_{n=0}$	0.26_1	0.60_1	[18]
	$Fe_{n=1}$	0.42_1	0.70_1	
	$Fe_{n=2}$	0.23_1	0.35_1	
	$Fe_{n=3}$	0.06_1	0.04_2	
	Fe I	−0.07†	0.081†	[19]
	Fe II	0.180†	0.466†	
	Fe III	0.278†	0.730†	

† Average values of the Gaussian distribution.

Two amorphous phases reported by Gaffet *et al* [5] (one of which should correspond to an amorphous silicon phase and another which has not been identified yet) were not observed, probably because under the present experimental conditions this step has been avoided.

The formation even at room temperature of unidentified highly disordered silicides after MBE iron deposition on Si(111) has been observed [21]. After annealing, this silicide transforms into CsCl–FeSi and finally into ε-FeSi. In our case, the occurrence of ε-FeSi could be related to the initial grown of a disordered silicide (not detected) that evolved into ε-FeSi under mechanical energy supply. The formation of ε-FeSi may be due to its more negative enthalpy of formation ($\Delta H = -26$ kJ mol^{-1} [22]) in comparison to that of $FeSi_2$ ($\Delta H = -12$ kJ mol^{-1} [22]). Once the $FeSi_2$ local atomic concentration is reached, driven by the global composition, β-$FeSi_2$ and α-$FeSi_2$ phases could be formed.

The presence of the metastable α-$FeSi_2$ phase can be understood by considering a deviation from the ideal stoichiometry and/or the defects created by the process itself. Moreover, the formation of α-$FeSi_2$ under non-equilibrium conditions has been reported several times, e.g. for single-crystal Si implanted with Fe ions at room temperature with subsequent ion-beam-induced epitaxial crystallization [10], rapid thermal annealing [23] and molecular beam epitaxy [24], or in ion beam mixing experiments [2, 3].

One difference between the present results and those of reference [25] is the observed stability of the β-$FeSi_2$ phase, which under milling did not decompose into ε-FeSi. This difference is still an open question.

Annealing at 1173 K for four hours induces order which is detected by a narrowing in the XRD and Mössbauer lines (figures 1 and 3). The x-ray diffraction patterns indicate that the majority phase is β-$FeSi_2$, α-$FeSi_2$ completely disappears and only traces of ε-FeSi are present. The Mössbauer spectra can be satisfactorily reproduced with the following quadrupolar interactions: I_1: $\Delta_1 = 0.60_1$ mm s^{-1}, $\delta_1 = 0.06_1$ mm s^{-1}, $F_1 = 41_1\%$; I_2: $\Delta_2 = 0.28_1$ mm s^{-1}, $\delta_2 = 0.07_1$ mm s^{-1}, $F_2 = 42_1\%$; and I_3: $\Delta_3 = 0.50$ mm s^{-1}, $\delta_3 = 0.28$ mm s^{-1}, $F_3 = 16_1\%$) associated with the non-equivalent iron sites in the β-$FeSi_2$ structure [8] and (with minor intensity) with ε-FeSi [13, 14]. The α-$FeSi_2$-to-β-$FeSi_2$ transformation is clearly observed in the diffractograms and in the Mössbauer spectra. Annealing at the same temperature for 12 h did not modify the phase contribution.

The effect of the replacement of Fe atoms by Pt atoms in $Fe_{1-x}Pt_xSi_2$ samples subjected to 19 h of mechanical alloying was also studied. Substantial changes are not observed in the main features of the XRD and Mössbauer results (see figure 4). However, even for the smallest Pt concentration used in the present investigation, lines belonging to Pt silicides are detected in the diffractograms. These lines can be associated with $Pt_{12}Si_5$, Pt_6Si_5 and PtSi together with those of β-$FeSi_2$, α-$FeSi_2$ and ε-FeSi. The contribution of Pt silicides to the diffractograms increases with Pt concentration. As regards the Mössbauer results, changes are not observed either in the neighbourhood of the Fe probes, or in the relative fractions (see table 3). After annealing at 1123 K for 4 h, an ordering is observed (see figure 5 and table 4), together with the α-$FeSi_2$-to-β-$FeSi_2$ transformation.

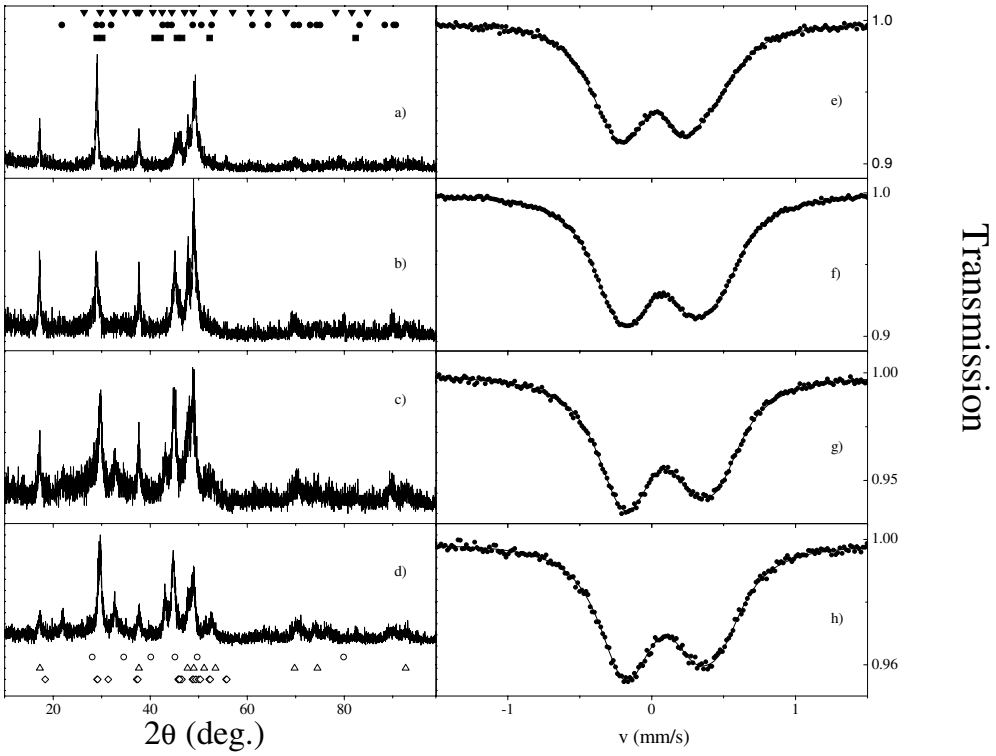

Figure 4. On the left, x-ray diffractograms taken from samples with different Pt concentrations milled for 19 h. On the right, the corresponding Mössbauer spectra. (a), (e) $x = 0.03$; (b), (f) $x = 0.09$; (c), (g) $x = 0.24$; (d), (h) $x = 0.36$. The open circles, triangles and diamonds indicate the positions of the lines belonging to ε-FeSi, α-$FeSi_2$ and β-$FeSi_2$, respectively. The solid triangles, circles and squares indicate the positions of the main lines of $Pt_{12}Si_5$, PtSi and Pt_6Si_5, respectively.

Using the method of atom location by channelling-enhanced microanalysis [6] and Mössbauer spectroscopy [26], it was confirmed that impurity preferentially occupies Fe sites. When the silicide is doped with Ni or Cr atoms, it was suggested from Mössbauer results that Ni atoms probably occupy site II while Cr atoms occupy site I [26]. However, these results should be checked, because the Mössbauer spectra were analysed using an old model of association between the measured hyperfine interactions and the structural sites [8]. In the case of Co doping, the Mössbauer results were not conclusive as regards a preferential replacement of Fe atoms by Co atoms [27]. The present Mössbauer results suggest that no significant replacement of Fe atoms by Pt ones in the structural sites of β-$FeSi_2$ has taken place. This hypothesis is

Table 3. Hyperfine parameters (Δ_i = quadrupole splitting, δ_i = isomer shift and Γ_i = linewidth) and relative fractions (F_i) obtained for $Fe_{1-x}Pt_xSi_2$ mixtures with different Pt concentrations milled for 19 h.

x	Δ_1 (mm s^{-1})	δ_1 (mm s^{-1})	Γ_1 (mm s^{-1})	F_1 (%)	Δ_2 (mm s^{-1})	δ_2 (mm s^{-1})	Γ_2 (mm s^{-1})	F_2 (%)
0.00	0.58_1	0.28_1	0.41_1	49_2	0.53_1	0.10_1	0.42_1	51_2
0.03	0.58_1	0.27_1	0.43_2	33_3	0.50_1	0.09_1	0.40_1	67_4
0.06	0.58_1	0.27_1	0.42_1	45_2	0.51_1	0.10_1	0.4_1	55_2
0.09	0.58_2	0.28_1	0.41_1	49_2	0.53_1	0.10_1	0.40_1	51_2
0.12	0.58_1	0.28_1	0.40_1	42_3	0.51_1	0.10_1	0.40_1	58_3
0.24	0.62_1	0.29_1	0.40_1	36_5	0.54_1	0.15_1	0.45_1	64_7
0.36	0.62_1	0.29_1	0.39_2	37_6	0.54_1	0.15_1	0.44_1	63_8
0.50	0.61_1	0.27_1	0.40_1	47_4	0.49_1	0.12_1	0.43_2	53_8

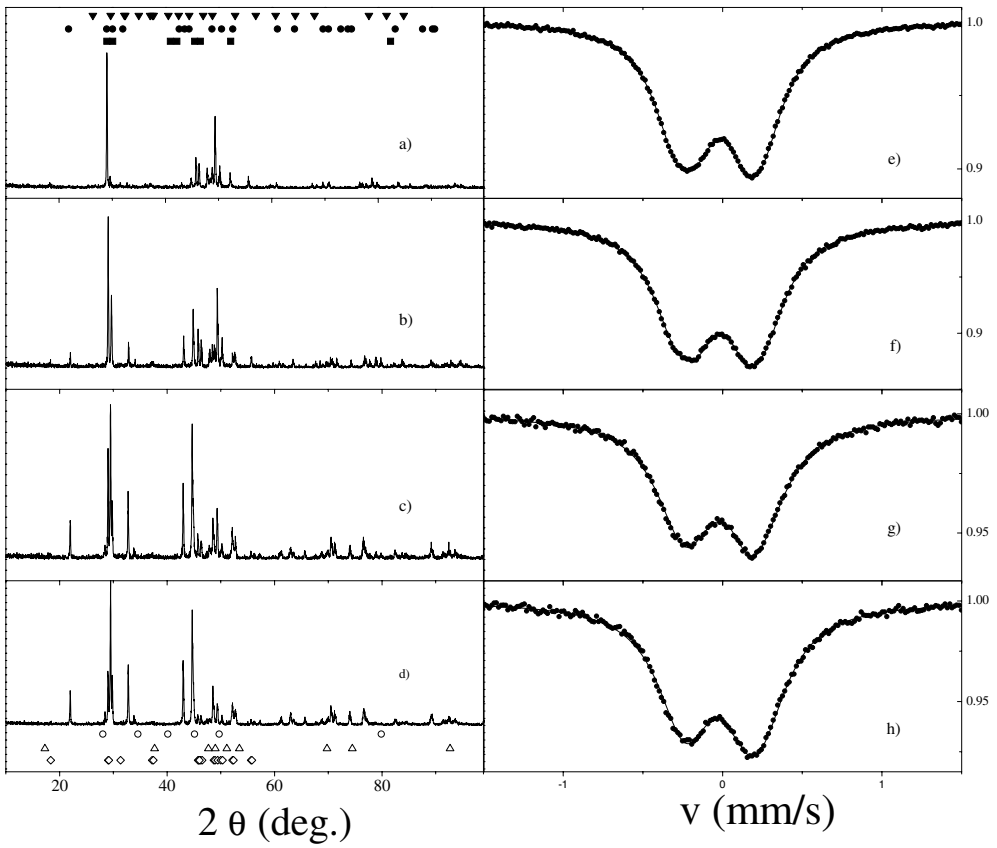

Figure 5. On the left, x-ray diffractograms taken from samples with different Pt concentrations milled for 19 h and annealed at 1173 K for 4 h. On the right, the corresponding Mössbauer spectra. (a), (e) $x = 0.03$; (b), (f) $x = 0.09$; (c), (g) $x = 0.24$; (d), (h) $x = 0.36$. The open circles, triangles and diamonds indicate the positions of the lines belonging to ε-FeSi, α-$FeSi_2$ and β-$FeSi_2$, respectively. The solid triangles, circles and squares indicate the positions of the main lines of $Pt_{12}Si_5$, PtSi and Pt_6Si_5, respectively.

supported by the fact that the populations of the two non-equivalent Fe sites in the β-$FeSi_2$ structure remain unchanged and equal to 50% as in the pure phase [8], as well as by the fact

Table 4. Hyperfine parameters (Δ_i = quadrupole splitting, δ_i = isomer shift and Γ_i = linewidth) and relative fractions (F_i) associated with $Fe_{1-x}Pt_xSi_2$ samples with different Pt concentrations milled for 19 h and annealed at 1173 K for 4 h.

x	Δ_1 (mm s^{-1})	δ_1 (mm s^{-1})	Γ_1 (mm s^{-1})	F_1 (%)	Δ_2 (mm s^{-1})	δ_2 (mm s^{-1})	Γ_2 (mm s^{-1})	F_2 (%)
0.00	0.60_1	0.06_1	0.33_1	41_1	0.28_1	0.07_1	0.32_1	42_1
0.03	0.56_1	0.08_1	0.32_1	47_6	0.33_1	0.09_1	0.33_1	51_6
0.06	0.56_1	0.08_1	0.32_1	50_4	0.32_1	0.09_1	0.32_1	47_4
0.09	0.57_1	0.08_1	0.33_1	48_7	0.32_2	0.09_1	0.33_1	45_7
0.12	0.56_1	0.07_1	0.33_1	46_4	0.32_1	0.09_1	0.30_2	48_4
0.24	0.54_2	0.07_1	0.34_1	45_{12}	0.34_3	0.09_1	0.31_2	41_{11}
0.36	0.57_2	0.07_1	0.33_1	36_8	0.33_2	0.09_1	0.31_2	42_7
x	Δ_3 (mm s^{-1})	δ_3 (mm s^{-1})	Γ_3 (mm s^{-1})	F_3 (%)				
0.00	0.50	0.28	0.30_1	16_1				
0.03	0.50	0.28	0.23_3	2_1				
0.06	0.50	0.28	0.30_2	3_1				
0.09	0.50	0.28	0.48_2	7_1				
0.12	0.50	0.28	0.48_1	6_1				
0.24	0.50	0.28	0.47_1	15_3				
0.36	0.50	0.28	0.49_1	21_3				

that the resulting hyperfine parameters do not change with Pt content. The segregation of Pt silicides under the present experimental conditions could be related to their highly negative heat of formation ($\Delta H_{PtSi} = -56$ kJ mol^{-1} and $\Delta H_{Pt_2Si} = -47$ kJ mol^{-1} [22]) compared with those of Fe silicides and, hence, the predominance of chemical forces.

4. Conclusions

The Fe–Si system ($FeSi_2$ composition) has been subjected to ball milling in order to investigate the sequence of phase formations and the silicide formation kinetics. According to the present results, the formation of iron silicides is a diffusion-controlled process with decreasing nucleation rate. The first end product is ε-FeSi and, as milling time proceeds, β-$FeSi_2$ and α-$FeSi_2$ are also formed. This sequence of phase formations is consistent with the heats of formation of the respective silicides and with the presence of defects created by the ball milling itself.

As regards the doping of β-$FeSi_2$ with Pt, the replacement of Fe atoms by Pt ones in the metal sites of β-$FeSi_2$ was not observed even for the lower Pt concentration studied. This could be related to the highly negative heat of formation of Pt silicides as compared with those of iron silicides.

The present results indicate that the chemical driving forces dominate over the mechanically induced non-equilibrium mechanisms under the present experimental conditions.

Acknowledgments

This work was partially supported by PICT 0201 of Consejo Nacional de Investigaciones Científicas y Técnicas (CONICET), and PICT 1277 of Agencia Nacional de Promoción Científica y Técnica, Argentina.

References

[1] Gupta A, Gupta R, Principi G, Jamitti E, Tossello C, Gratton L M, Lo Russo S, Rigato V and Frattini R 1992 *Surf. Coating Technol.* **51** 451
[2] Santos D L, de Souza J L, Amaral L and Boudinov H 1995 *Nucl. Instrum. Methods* B **103** 56
[3] Phase D M, Godbole V P, Kulkarni V N, Ghaisais S V, Ogale S V and Bhide V G 1987 *Nucl. Instrum. Methods* B **19/20** 737
[4] Umemoto M, Shiga S and Raviprasad K 1996 *Mater. Sci. Forum* **225–227** 841
[5] Gaffet E, Malhouroux N and Abdellaoui M 1993 *J. Alloys Compounds* **194** 339
[6] Hasaka M, Morimura T, Harano T and Kondo S 1995 *Mater. Charact.* **35** 195
[7] Dusausoy P Y, Protas J, Wandjii R and Roques R 1971 *Acta Crystallogr.* B **27** 1209
[8] Fanciulli M, Rosenblad C, Weyer G, Svane S and Christensen N E 1995 *Phys. Rev. Lett.* **75** 1642
[9] Joint Committee on Powder Diffraction Data 1966 *Powder Diffraction Files* (Atlanta, GA: Georgia Institute of Technology)
[10] Desimoni J and Sánchez F H 1999 *Hyperfine Interact.* **122** 277
[11] Christian T W 1965 *Theory of Transformation in Metals and Alloys* (Oxford: Pergamon) p 525
[12] Philibert J 1991 *Atom Movements Diffusion and Mass Transport in Solids* (Les ulis: Les Editions de Physique)
[13] Vojtyzechovsky K and Zemcik T 1974 *Czech. J. Phys.* B **24** 171
[14] Werthein G K, Wernick J H and Buchaman D N E 1966 *J. Appl. Phys.* **37** 3333
[15] Fanciulli M, Rosenblad C, Weyer G, Svane S and Christensen N E, von Känel H and Rodriguez C O 1997 *J. Phys.: Condens. Matter* **9** 1619
[16] Blaauw C, van der Woude F and Sawatzky G A 1973 *J. Phys. C: Solid State Phys.* **6** 2371
[17] Helgason O and Sigfüsson I 1989 *Hyperfine Interact.* **45** 415
[18] Fanciulli M, Rosenblad C, Weyer G, von Kanel H and Onda N 1996 *Thin Solid Films* **275** 8
[19] Sánchez F H and Desimoni J 1997 *Hyperfine Interact.* **110** 199
[20] Schwartz R B, 1997 *Proc. Int. Symp. on Mechanically Alloyed, Metastable and Nanocrystalline Materials* p 665
[21] Degroote S, Kobayashi T, Dekoster J, Vantomme A and Langouche G 1994 *Mater. Res. Soc. Symp. Proc.* **337** 685
[22] Boer F R, Boom R, Mattens W C, Miedema A R and Niessen A K 1988 *Cohesion in Metals* (Amsterdam: North-Holland)
[23] Reuther H, Weiser E, Panknin D, Grötzschel R and Skorupa W 1992 *Nucl. Instrum. Methods* B **68** 241
Reuther H and Dobler M 1996 *Surf. Interface Anal.* **24** 411
Dobler M, Reuther H, Betzl M, Mäder M and Möller W 1996 *Nucl. Instrum. Methods* B **117** 117
Dobler M, Reuther H, Betzl M and Mäder M 1995 *Proc. Int. Conf. on the Applications of the Mössbauer Effect* p 687
[24] Fanciulli M, Rosenblad C, Weyer G, von Kanel H and Onda N 1996 *Thin Solid Films* **275** 8
[25] Fernández Van Raap M B, Sánchez F H and Mendoza Zélis L A 1996 *Mater. Sci. Forum* **225–227** 383
[26] Kondo S, Hasaka M, Morimura T and Miyajima Y 1993 *Nucl. Instrum. Methods* B **76** 383
[27] Szymaski K, Dobrzinskiy L, Andryczuck A, Chrenowing R, Vantomme A, Degroote S and Langouche G 1996 *J. Phys.: Condens. Matter.* **8** 5317